International Journal of Research in Engineering and Science (IJRES)
ISSN (Online): 2320-9364, ISSN (Print): 2320-9356
www.ijres.org Volume 11 Issue 12 ǁ December 2023 ǁ PP. 177-185

Experimental Study on Mechanical Properties of Grouted Pile-Ring Beam Node with Localized Steel Sleeve+Bolt Connection

Wang Weizhe[1]， Yuan Shiwei[1]
[*1] *University of Shanghai for Science and Technology，Shanghai，200093，China*

Abstract
In order to solve the problem of grouted pile-ring girder node connection in pile-column integration, a grouted pile-ring girder node with localized steel sleeve + spigot connection is designed. The mechanical properties of the node are investigated by designing specimens of the node to be tested in the field by static loading method to verify the displacement of the crossbeam and ring beam of the node, the crack development process, and the strain of the reinforcement under different levels of loading. The test results show that the interface between the grouted pile and the ring girder did not slip significantly, and the interface connection is reliable. The damage of the specimen occurs in the combined part of the ring beam at the beam end. Plastic hinge was formed at the end of the beam, which is a ductile damage, and the longitudinal bars on the outer side of the ring girder were tensile to yield. The cracking load of the specimen was 30t, and the damage load was 110t. The results of the study can provide reference for the problem of the node connection of the pile-ring beam and promote the engineering application of the node connection of the beam-column in the pile-column integration.

Keywords: *reverse engineering； integrated pile-column:； cast-in pile-ring beam node:； localized steel sleeve + bolted connection:； mechanical properties.*

Date of Submission: 14-12-2023 Date of acceptance: 28-12-2023

I. INTRODUCTION

In the context of urban renewal, it is a feasible method to add a basement underneath an existing building by the reverse engineering method. By using the low-clearance bored piles technology in narrow indoor environments developed at the present stage, it can avoid the problems of large self-weight load, dense pile spacing, and excessive number of piles of the existing building, and improve the stability and bearing capacity of foundations on the basis of optimal use of the indoor space at the same time. Therefore, in this paper, the ring-beam node inverse method of "pile-column integration" is adopted to solve the difficulty of adding basement under the existing building [1-6].

In recent years, scholars at home and abroad have carried out a large number of experimental studies around the ring beam node of reinforced concrete columns. In 2019, Long Min[, Guangzhou University, Guangzhou, China] carried out a study on the application of the ring beam stiffness criterion to discretely braced shells under integral shear and bending. Long Min[7], Guangzhou University. proposed a new type of ring-beam node for reinforced concrete old columns and new beams connection, and the study concluded that the ring-beam node is excellent compared to other types of nodes in terms of reducing the construction difficulty and damage to the existing columns.2022, Renjun Yu [8], Chang'an University study aimed at proposing a new type of reinforced concrete cast-in-place piles (columns) - ring-beam node connection to reduce the construction difficulty and damage to the columns, and the study proposed a new type of reinforced concrete pile (columns) - ring-beam connection node to reduce the construction difficulty and damage to the columns. The study aims to propose a new type of reinforced concrete cast-in-place pile (column)-ring-beam node to reduce the construction difficulty and damage to the columns, and the design method and structural measures of the ring-beam node of "pile-column-integrated" are proposed. In 2023，Ahmed A. Hamoda [9]discussed the behavior of reinforced concrete ring girders reinforced with sustainable materials. The results show that the use of sustainable materials and reinforcement techniques can significantly improve the strength and ductility of reinforced concrete ring girders. At present, most of the researches on beam-column nodes at home and abroad focus on the mechanical properties, seismic performance, bearing capacity and calculation methods of steel pipe concrete-beam-column nodes, while the researches on the mechanical properties of the cast pile-ring girder nodes are very rare. Most of the experiments on ring-beam nodes are conducted with finite element simulation analysis, which lacks the support of engineering practice and experimental results. In this experiment, a new type of connection is

proposed for the grouted pile-ring girder node connected by localized steel sleeve + spigot, and then the experimental results such as deflection,crack development and width, concrete strain distribution, and reinforcement strain distribution of the ring girder structure are derived from the field in-situ tests [10].

1.1 Test piece design

According to the need of the project, the design load of the single crossbeam at the node is 70 T. The specimen was designed in this test for the infilled pile-ring girder node. The dimensions of the specimens (mm) are shown in Figure 1, and the reinforcement is shown in Table 1 and Figure 2.

(a) Elevations **(b) Floor plans**

Figure 1： Dimensional drawing of test piece

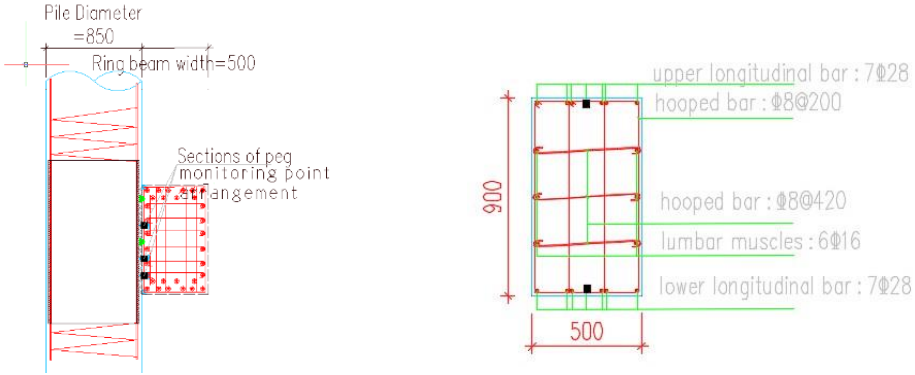

（a）Ring girder reinforcement （b）Cross beam reinforcement diagram

Figure 2： Dimensional drawing of test piece

Table 1： Specimen reinforcement table.

test piece	b/mm	h/mm	Upper longitudinal bar	Lower longitudinal reinforcement	hoop	lumbar muscle	tension bar
ring girder	500	1000	10Φ22	10C22	C14@280	C14@150	C14@560
crossbeam	500	900	5C28	5C28	A12@160	6A12	A12@320
			3C28	3C28			

1.2 Test piece production

Table 2： Table of specimen parameters

Specimen structure	Diameter D/mm	Height h/mm	Section size b x h (mm)2	Concrete strength class
grouted pile	850			C40
ring girder	1850	1000		C35
crossbeam			500 x 900	C35

Table 3：Material properties of reinforcing steel.

Reinforcing steel type	Diameter D/mm	Yield strength fy /(N/mm)2	Ultimate strength fst /(N/mm)2	use
HRB400 (Class III C)	22	385.8	531.6	Ring girder longitudinal reinforcement
	14	377.9	519.8	Ring beam girders, tie bars
HRB400 (Class III C)	28	386.5	530.6	crossbeam reinforcement
HPB235 (Level 1A)	12	225.6	305.3	Cross beam hoop, girdle, tie bars
	19	228.7	328.9	peg

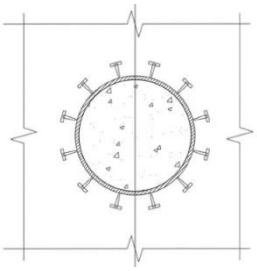

（a） **Welding of bolts on steel casing**

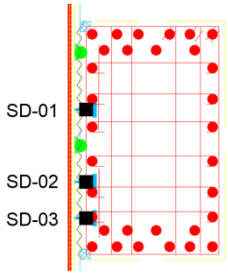

（b） **peg arrangement**

Figure3: Interface layout of steel sleeve + spigot connection

Figure 4:p Diagram of the test setup

Table 4: Table of test loading regimes.

load rating	Single Crossbeam Load/T	Single Crossbeam Cumulative load/T	Total cumulative load/T
first level	10	10	40
second level	10	20	80
third level	10	30	120
fourth level	10	40	160
fifth level	10	50	200
sixth level	10	60	240
seventh level	10	70	280
Eighth level	10	80	320
ninth level	10	90	360
tenth level	10	100	400
Eleventh level	10	110	440
...	...	...	...

1.3 Observation design

In the test, a total of 15 deformation observation points were arranged, and the deformation data were collected by using displacement sensors with a range of 30 mm, as shown in Figure 5. Among them, measurement points DP1, DP4, DP7 and DP9 are close to the inner edge of the ring girder and are used to observe the vertical deformation of the ring girder bonding surface. Measurement points DP2, DP5 are close to the outer edge of the ring girder, used to observe the vertical deformation of the outer edge of the ring girder.

DP3, DP6, DP8, DP10 are located at the loading point of the cross girder, used to observe the vertical deformation at the loading point of the cross girder. Measurement points DP11, DP12, DP13 and DP14 are located at the base of the jack and are used to observe the vertical deformation at the bottom of the jack. DP15 is located on the surface of the reaction beam and is used to observe the deformation at the bottom of the reaction beam.

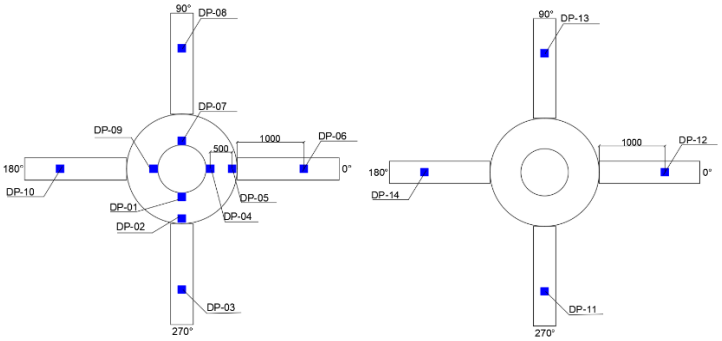

（a）Ring girder + cross girder measurement points （b）Jack Base Measurement Points

Figure 5: Specimen deformation measurement point layout

1.4 Strain observations

In the test, a total of 18 hoop strain measurement points were arranged in the ring girder. Measurement points 0GX, 45GX and 90GX were used to observe the horizontal section strain of hoop reinforcement in different directions in the compression zone of the ring girder, while measurement points 0GY, 45GY and 90GY were used to observe the vertical section strain of hoop reinforcement in different directions in the ring girder, as shown in Figure 6 (a). A total of 12 ring girder longitudinal bar strain measurement points were arranged. Measurement points 0HY, 45HY and 90HY were used to observe the longitudinal bar strains of the ring girder in different directions, as shown in Figure 6(b).A total of 12 crossbeam longitudinal strain measurement points were arranged. Measurement points 0SY-S and 90SY-S were used to observe the upper skin longitudinal strain of the crossbeam in different directions, while measurement points 0SY-X and 90SY-X were used to observe the lower skin longitudinal strain of the crossbeam in different directions, as shown in Figure 6 (c). For the local steel sleeve + spigot connection specimen, nine additional spigot strain measurement points were arranged, as shown in Figure 6 (d). Measuring points 0SD, 45SD and 90SD were used to observe the strain of pegs in different directions.

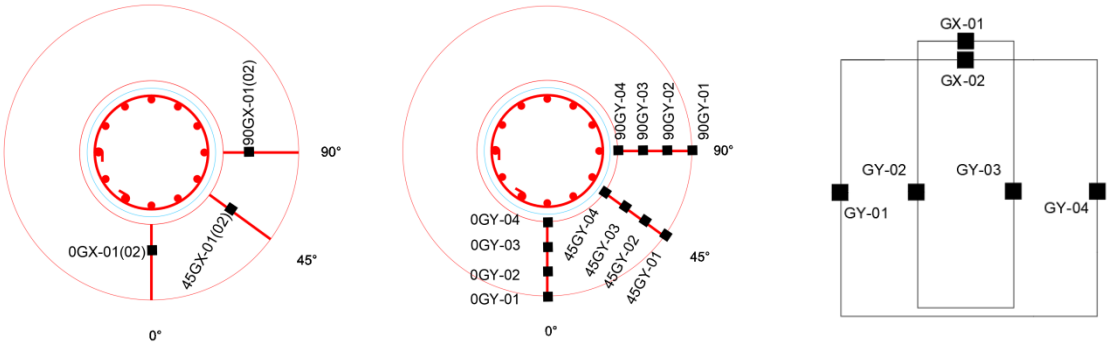

（a）Arrangement of hoop strain measurement points of ring beam

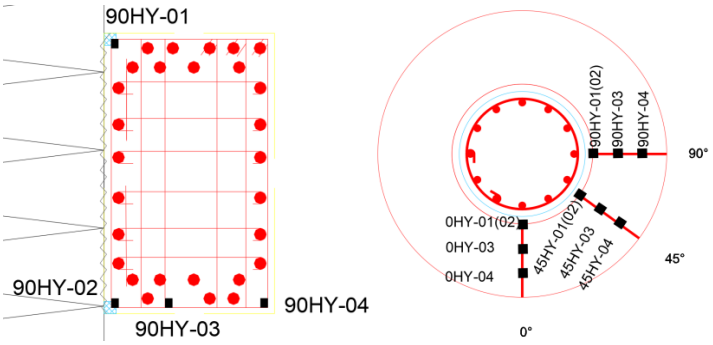

（b）Arrangement of Strain Measurement Points for Longitudinal Reinforcement of Ring Girder

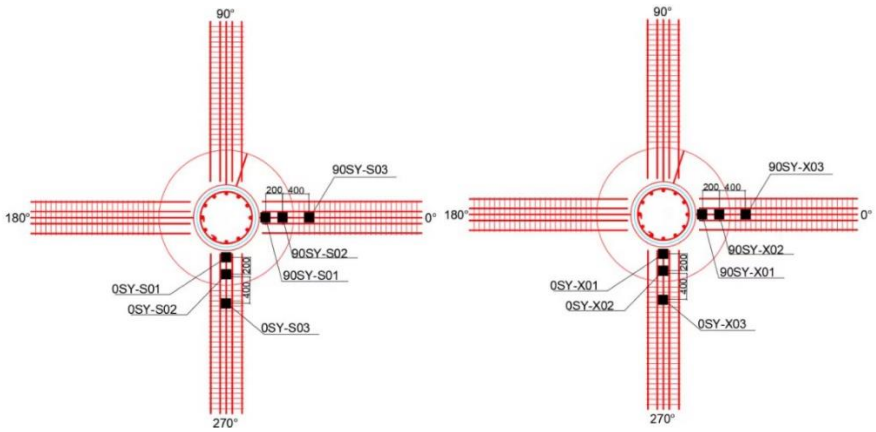

（c）Layout of strain measurement points on the upper (lower) surface of longitudinal bars of cross beams

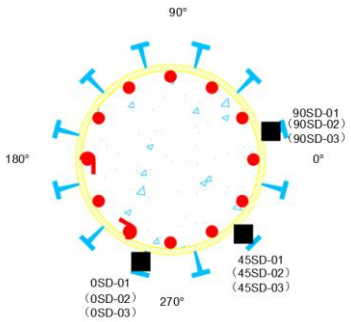

（d）Layout of pinned strain measurement points

Figure 6：Layout of test specimen reinforcement strain measurement points

II. RESULT AND DISCUSSION

The results obtained are as discussed below

2.1 Test phenomena and damage patterns

When the test load of single crossbeam reaches 30T, specimen cracks, and the diagonal crack at the lower edge of the junction of ring beam and crossbeam reaches 0.354mm, and the diagonal crack on the side of crossbeam reaches 0.343mm when the load reaches 60T. When the test load of single crossbeam reaches 70T, the diagonal crack on the side of ring beam runs through the top, and the transverse crack on the bottom surface of crossbeam appears and passes through. When the load reaches 80T, the diagonal crack on the side of the ring beam reaches 0.642mm, the diagonal crack on the side of the cross beam increases, the transverse crack on the bottom surface of the cross beam reaches 0.876mm, the crack on the bottom surface of the ring beam reaches 0.627mm, and the crack on the bottom edge of the junction between the side of the cross beam and the ring beam reaches 1.703mm. When loading a single crossbeam from 100T to 110T, the load could not be held, and the cracks on the surface of the specimen were distributed as follows: diagonal crack at the junction of the crossbeam and ring beam was 3.292mm, transverse crack at the bottom of the crossbeam was 2.612mm, radial crack at the bottom of the ring beam was 1.299mm, and transverse crack was 2.836mm. the test could not be carried out for the next level of loading, and the test was terminated. After observation, the concrete in the

pressurized area of the specimen was never crushed, and the interface between the ring beam and the grouted pile did not slip significantly.

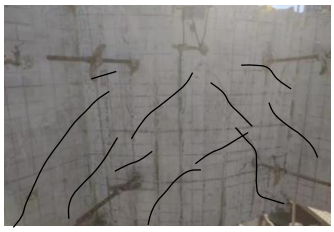

（a）**Ring beam side**

（b） **Cross beam side**

（c） **Ring girder to cross girder interface**

Figure 7：Final damage pattern of the specimen

2.2 Load-Displacement Curve Analysis

(i) The displacement of the jack base of the specimen during the whole test loading process is very small and negligible. The load-displacement curves at the loading point of the cross beams of the specimen are shown in Figure 8, and the overall displacement difference of the four cross beams varies very little, indicating that they basically deform synchronously.The displacement of the cross beams is very small and linear before 40t, and the specimen is in the stage of elastic change. Thereafter, the load-displacement curve increases nonlinearly. Eventually, when the 110t destructive load was reached, the maximum displacement at the loading point of the crossbeam was about 18mm, $\leqslant[\delta]=l_0/25=1000/25=40mm$,$l_0$ is the calculated span.

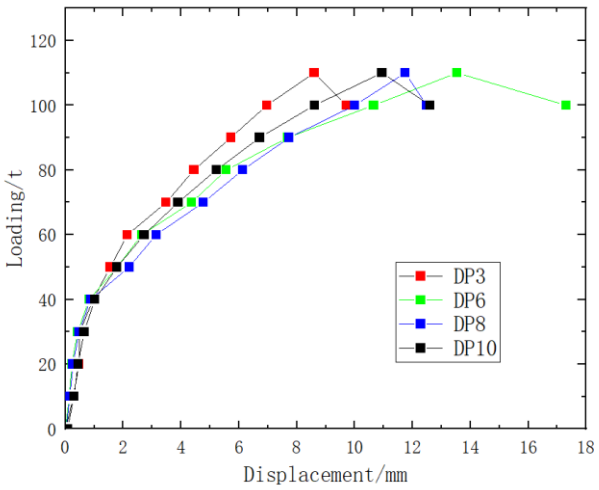

Figure 8: Load-displacement curve at the loading point of a cross beam

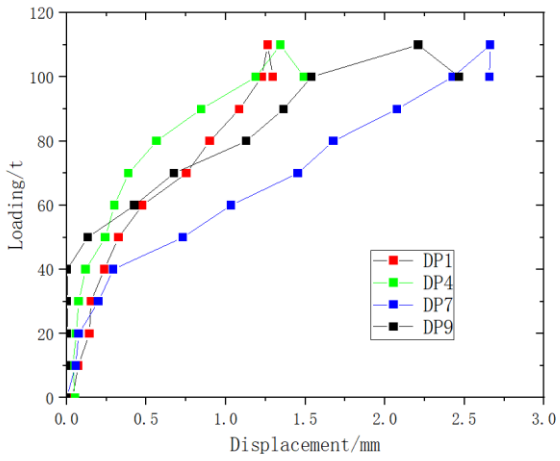

Figure. 9: Load-displacement curves of the ring-beam bond surface

(ii) As shown in Figure 9 , the overall displacement of the bonding surface was very small, and there was almost no displacement until 40T; thereafter, the load-displacement curve increased nonlinearly. Eventually, when 110T destructive load was reached, the maximum displacement at the ring girder bond surface was about 2.8mm.

(iii) As shown in Figure 10, the load-displacement curves of the outer edge of the ring beam at the two locations are slightly different, but overall both deformations are very small. Eventually, the maximum displacement of the outer edge of the ring girder was about 2.1mm when reaching the 110T destructive load.

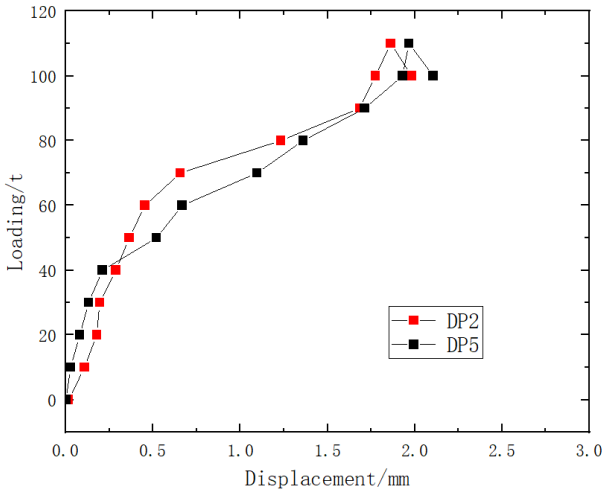

Figure. 10: Load-displacement curves at the outer edge of the ring girder

2.3 Load-strain curve analysis of reinforcing bars

The test results show that there is little difference between the load-strain curves of the reinforcement in each direction of the specimen, and the 0° direction is selected to plot the load-strain curve of the hoop beam reinforcement of the specimen.

(iv) As shown in Figure 11, there is basically no strain in the hoop reinforcement before 40 T, and the specimen is in the elastic stage, and the load is mainly borne by the concrete.After 40 T, the hoop reinforcement strain increases nonlinearly. Eventually, the longitudinal section of the outermost hoop bar (GY04) of the ring girder reached the yield state when the breaking load of 110T was reached. This observation highlights the important role of the hoop reinforcement in the ring girder during the test, especially the nonlinear strain behavior exhibited when carrying larger loads.

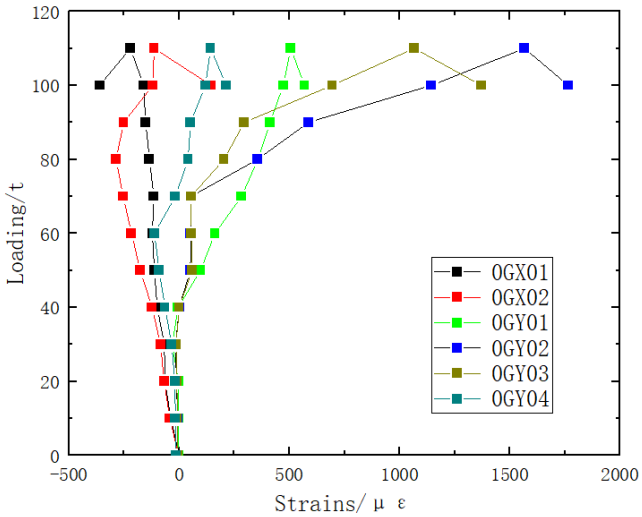

Figure. 11： Load-strain curve of hoop reinforcement of ring girder

(v) As shown in Figure 12, the longitudinal bar measurement point (HY01) on the upper surface of the ring girder was always in compression with negative strains, and the longitudinal bar measurement point on the lower surface was always in tension with positive strains.The hoop strain of the ring girder was very small before 40 T, and thereafter, the load-strain of the longitudinal bar of the ring girder increased nonlinearly. Eventually, the outermost longitudinal reinforcement (HY04) of the ring girder reached the tensile state and yielded when a breaking load of 110 T was reached. This observation emphasizes the apparent nonlinear response of the ring girder longitudinal bars during the stressing process, especially the yielding behavior as the damage load is approached.

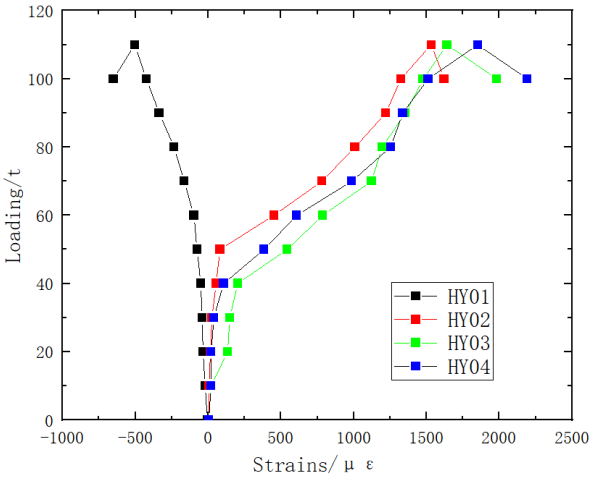

Figure. 12： Load-strain curve of longitudinal reinforcement of ring girder

(vi) As shown in Figure 13, the compressive strain of the longitudinal bars on the upper surface of the crossbeam was negative, and the tensile strain of the longitudinal bars on the lower surface was positive and increased nonlinearly. Eventually, before and after reaching the 110T damage load, the longitudinal reinforcement strain of the crossbeam appeared the inverse bending point, indicating that the longitudinal reinforcement of the crossbeam decreased in force after the damage of the specimen. It is noteworthy that none of the longitudinal bar strains of the cross beams eventually reached the yield point despite reaching the damage load. This observation emphasizes the nonlinear behavior of the cross beams in the tests, especially the deformation characteristics near the damage, and the failure of the longitudinal bars to reach the yield point.

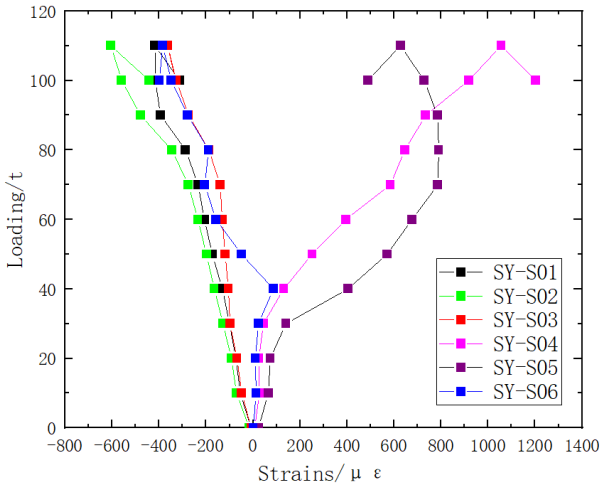

Figure. 13：Load-strain curve of longitudinal reinforcement of crossbeam

(vii) The peg load-strain curve of specimen A is shown in Figure 14 below. The middle peg (SD02) was loaded significantly more than the other two pegs (SD01, SD03).Before 40t, there was almost no strain in the pegs, and the structure was in the elastic deformation stage, and then the pegs' strain gradually increased in a nonlinear manner. Eventually, the strain of the pegs did not reach yield when the 110t destructive load was reached.

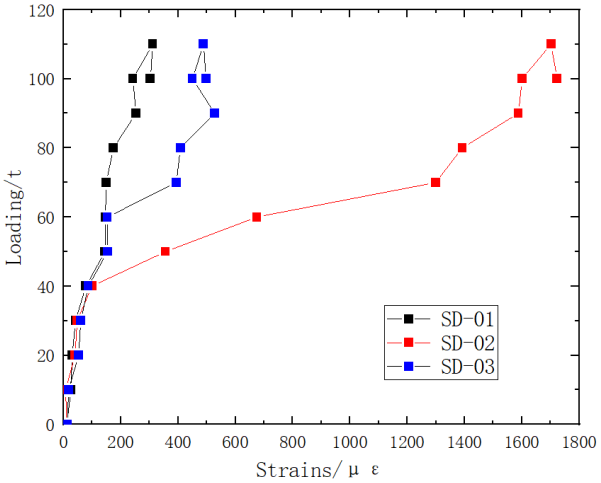

Figure. 14：Load-strain curve of pegs

III. CONCLUSION

(1) For the specimen with local steel sleeve + bolt connection, the overall deformation of the combined surface of the ring beam is small, the maximum deformation is about 2.8mm, and the interface between the pile and the ring beam has no obvious slip, and the interface connection is reliable.

(2) The maximum deformation of the specimen at the loading point of the crossbeam reaches about 18mm, which is less than the allowable deflection of 40mm. the specimen cracks when the load of the single crossbeam reaches 30t; the specimen is destroyed when the load reaches 110t. the load capacity of the specimen meets the design load capacity, and the specimen has no significant deformation. The load capacity of the specimen meets the design load capacity of 70t.

(3) The damage of the specimen occurs in the combined part of the ring beam at the beam end. Plastic hinge is formed at the beam end, which belongs to ductile damage, and the longitudinal bars on the outer side of the ring girder are tensile to yield.

REFERENCES

[1]. Zhang Puyang, Bai Yu, Liu Yang, Xu Yunlong, Ding Hongyan. Structural Performance of LNG Concrete Storage Tank Wall-Ring Beam Nodes [J].Industrial Construction,2022,52(08):127-131+174.

[2]. Feng Yu,Zekang Song,Iman Mansouri,Jie Liu,Yuan Fang. Experimental study and finite element analysis of PVC-CFRP confined concrete column – Ring beam joint subjected to eccentric compression[J]. Construction and Building Materials,2020,254(C).

[3]. Metals Research; Study Findings from China University of Mining and Technology Provide New Insights into Metals Research (Seismic behaviors of ring beams joints of steel tube-reinforced concrete column structure)[J]. Journal of Technology & Science,2018.

[4]. Bingqing Dong,Jinlong Pan,Jingming Cai,Togay Ozbakkaloglu. Mechanical Behaviour of ECC Ring Beam Connections under Square Local Compressive Loading[J]. Journal of Building Engineering,2020,34(prepublish).

[5]. Xiaodan Fang, Research on key technology of steel pipe concrete column ring beam node. Guangdong Province, South China University of Technology, Architectural Design and Research Institute, 2017-06-16.UOP (1990) "Linear Detergent Alkylation Unit, General Operating Manual" pp. 1 –610.

[6]. LU Wenlong, SHEN Zhaoyong, LONG Min. Experimental study on new ring-beam type node of reinforced concrete old column-new beam connection and its seismic performance[J]. Industrial Building,2019,49(4):187-190+186.

[7]. Long Min. Experimental study on the seismic performance of a new ring-beam node with reinforced concrete old column and new beam connections [D]. Guangzhou: Guangzhou University, 2019.

[8]. Yu Renjun. Research on mechanical properties of concrete-filled pile (column)-ring beam node [D]. Xi'an: Chang'an University, 2022.

[9]. Ahmed A. Hamoda, Boshra A. Eltaly, Mohamd Ghalla, Qing Quan Liang,Behavior of reinforced concrete ring beams strengthened with sustainable materials,Engineering Structures,Volume 290,2023,116374.

[10]. WAI Hong,CHEN Timming,LIU Qinghui. Static experimental study and design method of reinforced concrete beam-square steel pipe concrete column ring beam node[J]. Journal of Building Structures,2013,34(01):76-84.